Electric Power Systems Research 169 (2019) 195–205

Contents lists available at ScienceDirect

Electric Power Systems Research

journal homepage: www.elsevier.com/locate/epsr

Differential protection for stator ground faults in a full-converter wind turbine generator

Rodrigo P. Bataglioli[a], Renato M. Monaro[b,*], Denis V. Coury[a]

[a] São Carlos School of Engineering – University of São Paulo,SP, Brazil
[b] Polytechnic School – University of São Paulo, SP, Brazil

ARTICLE INFO

Keywords:
Discrete Fourier Transform
Full-scale power converter
Real time digital simulator
Stator winding protection
Wind generator

ABSTRACT

Consolidated schemes and philosophies have been developed for Wind Energy Conversion Systems (WECS) protection. Although various studies have addressed this topic, including the internal protection function, there is still room for improvement, for instance, concerning the use of differential logic under varying frequencies. An aggravating factor related to protection issues is the high penetration of electronic devices in recent topologies, which may result in different responses in the case of internal faults, depending on the control strategy. In this scenario, conventional protection may not work properly. Based on this and considering the increasing tendency towards using full-converter WECS, there is a need to standardize them as well as improve their protection schemes. Thus, this paper analyses the application of the differential function in order to detect internal faults in a full-converter wind turbine generator. A differential protection scheme based on Discrete Fourier Transform (DFT) using dynamic window was discussed in this paper. The main objective was to reduce the phasor estimation error caused by the stator frequency variation. A complete protection scheme was implemented and tested using fault simulations from a Real Time Digital Simulator (RTDS). Very promising results were obtained. Furthermore, it was demonstrated throughout the paper that the grounding configuration greatly influences the protection performance of such equipment.

1. Introduction

Wind energy generation has grown considerably in recent years. In 2015, more than 63 GW were installed, reaching a global total of approximately 433 GW [1]. From this total, the countries with the largest installed wind farms are China, USA and Germany with approximately 145, 74 and 45 GW, respectively. By the end of 2020, it is expected that 12% of the world's electricity demand will be supplied by wind power plants [2]. The forecast is that by consolidating smart grids, installed wind power capacity will increase even further [3]. This underscores the importance of research in this form of generation.

There are several schemes to connect the Wind Energy Conversion Systems (WECS) to the Electric Power System (EPS), such as direct connection, the Doubly Fed Induction Generator (DFIG) and using a full-scale power converter [4]. Each type of connection is related to the classification of the turbine as fixed or variable speed [5]. In the case of fixed speed turbines, the rotor speed is coupled to the grid frequency. This configuration is subject to a higher mechanical stress during wind gusts. In contrast, applying power converters to variable speed turbines allows the rotor speed to change according to the wind speed, which results in a better energy extraction from the wind if a maximum power point tracking (MPPT) control is used.

Regarding the WECS operation, each topology has intrinsic characteristics that may result in different behaviors in case of internal faults, especially those with a high penetration of power electronics that are influenced by the control strategy. Among these, the full-converter wind turbine generator has been one of the mostinstalled, reaching 40.8% of the global market in 2013, from which 89.95% was consisted of synchronous machines [6].

Thus, despite the failure rate in rotating machines being low for new designs with improved materials, internal faults still occur, and if there are excessive time delays in the trip signal or blind spots in the protection, the fault can result in serious damage and long interruptions in the generation unit operation in order to repair the machine [7]. As generators are subject to more types of faults than any other device, there are several protection philosophies applied to synchronous generators (SGs).

However, consolidated protection schemes and philosophies have been developed for conventional applications, such as hydroelectric and thermoelectric generation units [8]. Hence, if conventional

* Corresponding author
E-mail addresses: rodrigo.bataglioli@usp.br (R.P. Bataglioli), monaro@usp.br (R.M. Monaro), coury@sc.usp.br (D.V. Coury).

https://doi.org/10.1016/j.epsr.2018.12.018
Received 20 March 2018; Received in revised form 27 November 2018; Accepted 21 December 2018
Available online 11 January 2019

functions are applied improperly, the output can result in economic and material damage to consumers and to the EPS itself. An aggravating factor is that the failure rate in wind units is higher as its installation is subject to severe environmental conditions [9].

Ever increasing interest in the protection of wind power applications can be observed by the growing number of publications that address this topic. Some of these studies are presented as follows.

Conroy and Watson [10] investigate the low-voltage ride through (LVRT) capacity of full-converter wind generators. It is demonstrated that, as the pitch control has a slow response, the reduction in the angle of attack does not present satisfactory results to limit the power extracted from the wind. Another solution would be to increase the DC link capacitance. However, because the capacitor size would depend on the undervoltage duration, this approach is impractical. Thus, this article presents an analysis of the connection of a resistor in the DC link through a DC/DC converter to dissipate surplus energy during external faults. Based on this, in order to solve problems related to the overheating of the resistor and switches, the authors proposed the combination of pitch control with this technique.

Khoddam and Karegar [11] show an analysis of the impact caused by wind power plants equipped with DFIG on their transmission line protection. The results were obtained for the case of faults in a transmission line involving phase A to ground. They verified that the characteristics of a wind farm, such as variations in load, voltage levels and impedance of wind turbines, significantly affect the limits of the distance relay. Based on this observation, they concluded that distance relays with fixed adjustments are not suitable for the protection of transmission lines that connect wind farms to the electrical system.

Zheng et al. [12] describe a protection algorithm for wind turbines operating in a large wind farm. The algorithm is based on the magnitude of the positive sequence current to discriminate terminal faults in a generator connected to the same feeder from a fault in an adjacent busbar. In order to distinguish between a fault at the protected generator terminal or at the feeder itself from a fault in the tie or grid, the phase angle of the negative sequence current was used to determine the fault type and the magnitude of the positive sequence current to decide between an instantaneous or timed operation.

Kusiak and Li [13] developed a methodology to predict faults based on the application of data mining based algorithms in a bank of fault oscillographs registered by the supervisory system of a wind farm. The methodology consists of 3 levels: identification, severity and classification. The results showed that in most cases the fault can be predicted 60 minutes in advance and a reasonable accuracy of about 90% in one of the tests. However, because the database used is limited, not encompassing all types of faults, the fault classification is less efficient.

Gkavanoudis and Demoulias [14] propose the connection of a supercapacitor bank in the DC link to meet the requirements of LVRT and to allow the output power smoothing control. This approach establishes that, in the case of a fault in the grid, the surplus energy is stored in the storage system instead of being dissipated in the braking resistors (used in the traditional variable speed WECS topologies).

Mohapi et al. [15] present the modeling and simulation of an external fault protection based on a dynamic resistor in series for a wind generator composed by permanent magnet synchronous generators. The results indicate that the protection scheme is only effective when using a suitable switching control, otherwise the generator loses synchronization with the grid in case of a fault in the transmission line. The series dynamic resistor operates as follows: in case of normal operation, the bypass in parallel with the protection element remains closed, while the bypass is opened in the event of an external fault, thus the surplus energy is dissipated in the resistor.

Hooshyar et al. [16] reveal some serious shortcomings of distance protection for lines connected to wind farms during balanced faults. In particular, it has been found that the impedance measured at the terminals of a squirrel cage induction generator does not represent the true location of the fault a few cycles after a three-phase fault in one of the transmission lines, leading to an improper operation. A new scheme has been proposed to address this problem, which provides fast and non-timed protection for the entire line. In this scheme, the remote relay uses an extended impedance zone, while the wind farm substation relay detects the fault direction according to the properties of the current waveform. The technique is also based on the high decay characteristic of the fault current peak at the squirrel cage induction generator.

Mansouri et al. [17] provide an overview of the protection for DFIGs based wind turbine. Considerations of the conventional synchronous generator protection adapted to DFIG topology and the protection devices commonly used in this topology are presented. In addition, the authors propose three new schemes: differential protection for interturn fault protection, a new start-up and a synchronization method and protection coordination of overcurrent protection considering LVRT requirements. As in the DFIG topology the stator is normally connected through step-up transformers to the grid, many of the conventional protections described in the IEEE Guide C37.102-2006 [8] can be applied to it. However, the authors concluded that despite the rapid growth of technology, which has generated wind units in the order of MW, a comprehensive protection scheme for these components has not yet been presented and validated. Furthermore, it is important to note that the DFIG presents an operation characteristic quite different from the full-converter wind generator.

As presented above, although various studies address WECS protection, there is a lack of research regarding internal faults in a full-converter wind generator. Based on this and considering the increased tendency towards full-converter WECS penetration in the generation matrix, it is fundamental to standardize and revise its protection schemes. Therefore, this paper proposes using differential protection in order to detect internal faults in full-converter wind turbine generator based on SGs. Furthermore, all grounding configuration types are considered to verify the relay performance for each case, as it depends on the WECS manufacturer and has an influence on the internal fault behavior [18]. In order to address the variable frequency at the stator circuit, a dynamic window based on Discrete Fourier Transform (DFT) is implemented.

This paper is organized as follows: Section 2 analyzes the conventional differential stator winding protection applied to wind generators. Based on this, Section 3 describes the accuracy test and analysis of the DFT with fixed and dynamic windows using MATLAB® software and Section 4 presents the internal fault scenarios simulated in a real time digital simulator (RTDS) to verify the impact of the DFT algorithm and grounding configuration in the differential protection. Finally, Section 5 draws the conclusions about using this protection for a full-converter wind generator.

2. Conventional differential protection

Before applying this kind of protection to the wind generator, it is important to primarily understand its intrinsic limitations in order to understand the problems introduced by the wind generator operation.

Differential protection, function 87 according to ANSI, is the most commonly used method to protect the generator against stator faults. In normal operating conditions, the measuring currents per phase near the terminal and neutral of the machine are similar, disregarding current transformers (CTs) measuring errors. However, in case of faults within the protection zone defined by the CTs, the differential current increases, depending on the grounding configuration and internal fault location, which can result in the protection relay operation. Although this method is largely used in conventional protection, it has some limitations, such as:

- The influence of the generator operating point on the setting of the protection curves. The load current contributes to the restraint current of the differential relay, increasing the operating current

required to sensitize the relay and, thereby, decreasing the sensitivity of the differential protection [19].
- Inter-turn faults cannot be detected, because in this type of fault the input and output currents in the winding are the same [19].
- Depending on the grounding configuration, the generator neutral impedance may influence the ground fault protection. For example, considering a generator with wye-grounded stator winding connected to a transformer with delta winding, a high-impedance ground results in a larger unprotected portion of the winding close to neutral [8].
- In situations of high fault current and DC components, CTs are subjected to saturation, causing malfunction of the differential protection [20]. However, before specifying the CTs, a previous study must be carried out to guarantee that the saturation in fault situations does not occur [21]. Based on this, a differential protection based on instantaneous values may have some misoperation cases if CT saturation occurs, while the phasor-based functions are more immune to this type of problem.

The variable-speed wind turbine, based on a full power converter, presents extremely different characteristics from the conventional application. Therefore, adaptations in the protection functions are necessary.

Among the operational characteristics of this wind turbine topology, the following are highlighted:

- Variable electric frequency in the stator circuit;
- Electromechanical decoupling between the SG and the grid.

It is interesting to note that in the case of the topology known as DFIG, the stator circuit is normally connected through step-up transformers to the grid. In other words, the electric frequency in the stator circuit is not variable in this case. This is different from what occurs in the rotor circuit that is connected to the system by a partial power converter. Due to this configuration, the DFIG is not completely electromechanically decoupled from the electric system.

Based on the characteristics mentioned, an analysis of the differential protection was carried out, aiming to identify its limitations for wind generators based on full power converters.

A typical differential protection algorithm is represented by Algorithm 1 [22]. To summarize, the function is based on the current phasors measured near the machine's terminals: line ($\vec{I_1}$) and neutral ($\vec{I_2}$). A simple operating curve of differential (I_d) versus restraint (I_r) currents is defined by a pickup, adjusted according to CT inaccuracies, and a slope to cope with possible CT saturation errors caused by long lasting DC components, as well as high currents. A more complex curve, based on two pickups and two slopes, is presented in Fig. 1. This curve allows a better adjustment according to CT saturation errors relative to DC components (slope 1) and high currents (slope 2) [22,23].

Algorithm 1. Differential function

1: $I_d \longleftarrow |\vec{I_1} - \vec{I_2}|$
2: $I_r \longleftarrow \max(|\vec{I_1}|, |\vec{I_2}|)$
3: **if** (I_r, I_d) are above the operating curve **then**
4: **return** true
5: **else**
6: **return** false
7: **end if**

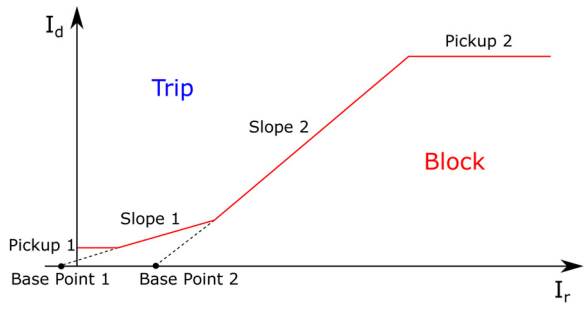

Fig. 1. Characteristic curve adopted for the differential protection [23].

The phasor calculation used by the differential function is illustrated by Algorithm 2, in which a full cycle DFT is conveniently used [24]. The parameters $\vec{I}$, n, N and $i(n)$ are, respectively, current phasor output, loop index, window size and a circular buffer with the latest N samples of the current signal.

Algorithm 2. DFT calculation

1: $\vec{I} \longleftarrow 0 + j0$
2: $n \longleftarrow 1$
3: **for** $n \leq N$ **do**
4: $\vec{I} \longleftarrow \vec{I} + i(n)e^{-\frac{2\pi}{N}nj}$
5: $n \longleftarrow n + 1$
6: **end for**
7: **return** $\frac{\sqrt{2}}{N}\vec{I}$

As presented above, the differential function input is the current phasors, obtained with the DFT. Thus, the commercial relays applied for full-converter generator protection need to be suitable for non-nominal frequency conditions. According to the manuals of two commercial relays, specific for the complete protection of synchronous generators, each current measurement system has the following allowed frequency ranges, in which the respective device is able to correctly estimate the phasors:

- **Relay 1:** 50 ± 10% or 60 ± 10% Hz;
- **Relay 2:** 20–65 Hz.

Based on these specifications, it can be said that not every relay available on the market is indicated to be applied in the protection of a full variable-speed wind generator, which has an operating frequency range according to the wind speed. It is noteworthy that even commercial relays with variable frequency phasor estimation requires further studies concerning the CT accuracy degradation with varying frequencies to be used in variable speed wind generator protection.

Although the user does not have access to the algorithms embedded in commercial relays, based on the manual specifications, it is possible to understand how the device works. Regarding relay 1 that has a restricted range of frequency variation, it can be concluded that a DFT algorithm was implemented based on a fixed window length. On the other hand, relay two possibly works with a dynamic window that varies according to the measured frequency.

Furthermore, considering a conventional generation unit, the typical grounding configurations are wye-grounded stator winding and delta transformer generator-side or delta stator winding and wye-grounded transformer generator-side. In contrast, the grounding configuration in a full variable-speed WECS has other technical aspects as the transformer and generator are separated by the back-to-back converter. This new paradigm may affect the differential protection performance.

Thus, the following section addresses the DFT analysis in order to show the differential function limitations considering full-converter wind generators.

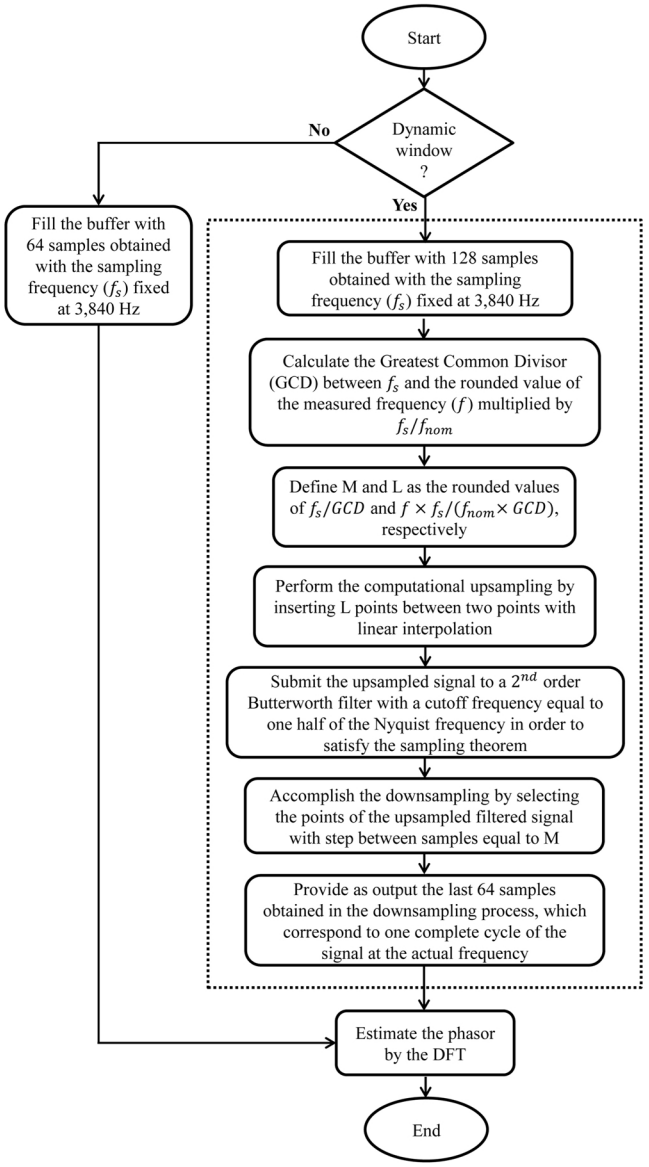

Fig. 2. Flowchart of the algorithm for fixed and dynamic windows based on DFT.

3. Discrete Fourier transform analysis

The procedure performed to obtain the accuracy of the DFT routine with fixed and dynamic windows, when submitted to frequency variation, is described next.

3.1. Fixed and dynamic window of the DFT comparison procedure

In order to evaluate the errors introduced by each window type in the phasor estimation, two algorithms were implemented in the MATLAB® R2015a software.

The first routine consists of a fixed window based on DFT that operates according to the flowchart illustrated in Fig. 2, disregarding the dashed part that refers to the dynamic window based DFT. Note that regardless of the signal frequency, the buffer contains 64 samples obtained with the same sampling frequency. Thus, if the frequency is different from the nominal (60 Hz), the data window will not contain an integer cycle of the fundamental component.

The second routine, also described in the flowchart presented in Fig. 2, used the concept of dynamic windows in order to overcome the limitation presented in the first one. Similar to the previous algorithm, the buffer size and sampling frequency do not vary. Therefore, the dynamic window is obtained using a computational resampling procedure of the stored data. Basically, the current buffer is upsampled by interpolating new samples (linear interpolation) according to the measured signal frequency. After that, the signal is filtered and downsampled in order to obtain a new buffer with 64 samples that represents a cycle of the current signal.

For the sampling frequency of 3840 Hz, a 128-sample buffer size represents 1 cycle of the wave when the signal frequency is 30 Hz. In other words, the minimum possible frequency to enable the phasor estimation depends on the buffer size and sampling frequency. On the other hand, the maximum frequency only depends on the sampling rate, i.e., the Nyquist theorem [25], which defines the cut-off frequency of the Butterworth filter as half of the sampling frequency. However, the higher the sampling frequency, the longer the processing time. Hence, it is important to choose a sampling rate satisfying the Nyquist theorem for the wind turbine operating range.

Based on the algorithms implemented, two analyses were made. One to determine the DFT accuracy in steady state, considering all operating points of the wind generator under analysis, and the other to inspect its dynamic response during a frequency ramp. The results obtained from the proposed methodology are reported below.

3.2. Fixed and dynamic window of the DFT comparison results

Considering the wind generation unit under analysis, which operates in the frequency range of 30–60 Hz, respectively the cut-in and nominal frequencies, the error curves versus frequency are illustrated in Fig. 3 for two signals with different phases. A logarithmic scale on the y-axis was adopted. The DFT algorithm, which has a dynamic window based on computational resampling, presents an extremely low amplitude error (below 0.2%) regardless of frequency, while the fixed window based DFT only performs a good accuracy around the fundamental frequency, in this case 60 Hz. Furthermore, for the algorithm with a fixed window, the amplitude and phase errors depend on the signal phase. This may affect the differential protection, as the currents' phases near the terminal and neutral of the machine differ during saturation and internal fault situations.

After the improved performance of a dynamic window has been proven, the DFT response to a frequency ramp should be investigated, simulating a wind speed variation. The DFT responses with fixed and dynamic windows for a frequency ramp of 10 Hz/s are shown in Fig. 4, considering a current signal of 300 A and 60 Hz. This condition is near the nominal operating point of the simulated wind generator, which is described in Section 4. During the ramp application, the amplitude estimated presents an oscillation that can be seen in a maximum peak-to-peak error, whereas the phase is apparently not affected. However, it can be observed that the steady state error is very small only for the dynamic window based DFT.

Table 1 shows the maximum peak-to-peak error for some frequency ramps, considering extreme cases. It can be inferred that the window types present errors of up to 6.6 and 4.5%, respectively, during the evaluated events, which grow according to the increase in the derivative of the frequency.

The analysis presented indicates that the commercial relay used in a full variable-speed wind generator must have a dynamic window based DFT in order to avoid improper trip signals and blind spots in the protection.

In order to analyze the impact on the differential protection performance of the DFT with a fixed window and also the grounding configuration, the next section describes the internal fault simulations using the RTDS® hardware.

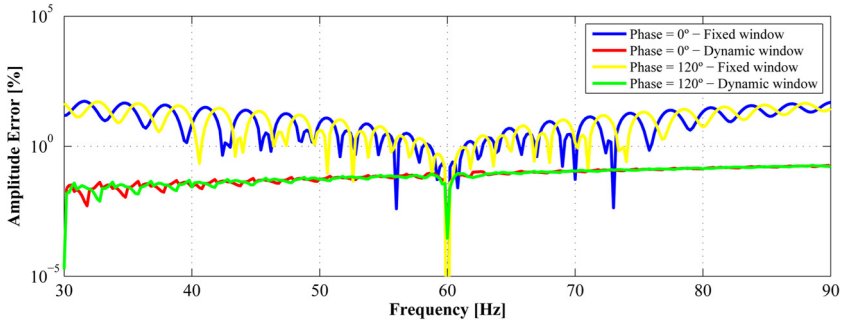

(a) Amplitude error.

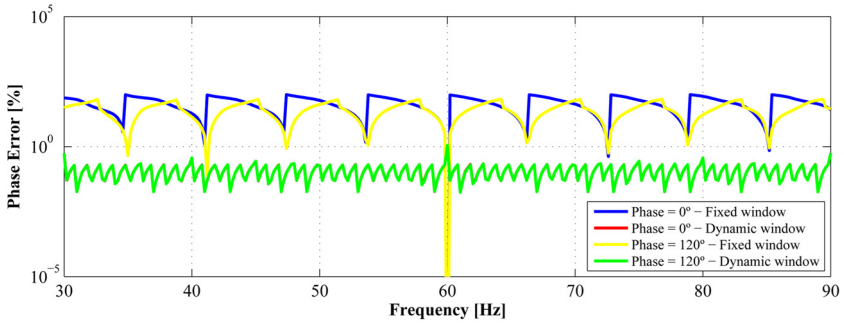

(b) Phase error.

Fig. 3. Error analysis in the phasors estimated by the DFT with fixed and dynamic windows.

4. Internal fault simulation analysis

The modeled system and the simulated internal fault scenarios are described in the sequence.

4.1. Simulation methodology

An EPS consisting of a full-scale power converter WECS connected to an equivalent grid, using a transformer and a line transmission, illustrated in Fig. 5(a), was modeled in the RSCAD software and simulated in the RTDS® hardware. This type of equipment reliably reproduces the conditions of an actual electrical system.

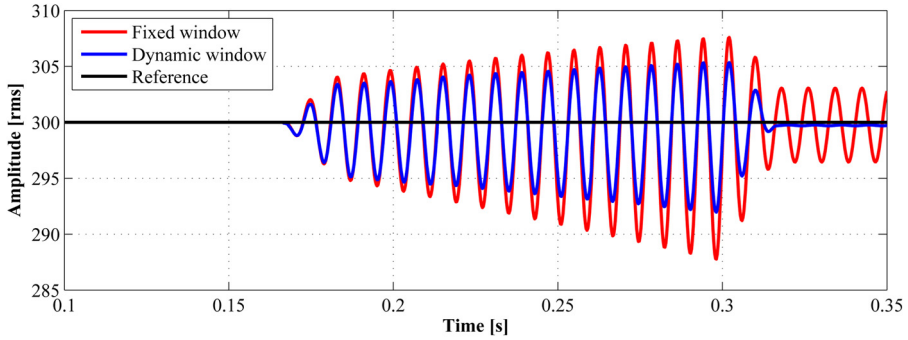

(a) Amplitude response.

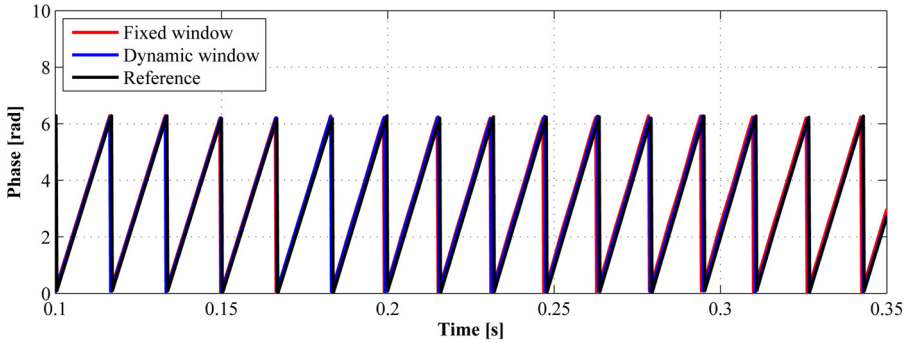

(b) Phase response.

Fig. 4. DFT response to a ramp of 10 Hz/s in the frequency.

Table 1
DFT error for some possible frequency ramp values.

Ramp [Hz/s]	Maximum peak-to-peak error [%]	
	Fixed window	Dynamic window
0.1	0.07	0.04
0.5	0.34	0.23
1.0	0.68	0.45
2.0	1.36	0.91
5.0	3.39	2.30
10.0	6.60	4.46

Table 2
Grounding configurations considered.

Scenario	Generator	Converter	WECS-side transformer terminals
1	–	–	–
2	Neutral grounded	–	–
3	–	NPC	–
4	Neutral grounded	NPC	–
5	–	–	Wye-grounded
6	Neutral grounded	–	Wye-grounded
7	–	NPC	Wye-grounded
8	Neutral grounded	NPC	Wye-grounded

The WECS is composed by a full variable-speed wind turbine, a 2 MVA Wound Rotor Synchronous Generator (WRSG) and a full-scale 3-level back-to-back voltage source converter (VSC). The system data is summarized in Appendix.

Concerning the full variable-speed WECS based on dq control [26], the grounding configuration affects the fault current behavior. As this configuration depends on the WECS manufacturer, the protection scheme will also depend on it. Therefore, it is important to consider its influence in the relay operation. The WECS grounding configuration, highlighted in Fig. 5, illustrates a solid grounded generator, a Neutral Point Clamped (NPC) converter and a wye-grounded WECS-side transformer connection. However, in order to analyze its impact in the differential relay operation, other configurations are simulated, as summarized in Table 2. For the grounded generator conditions, high and low neutral impedances were considered. The ground resistances considered are 0.01, 3.1 and 12.41 Ω [27].

The RSCAD SG model can vary the portion of the stator winding (A phase) under a short-circuit in the range of 5–95%, providing a relatively wide analysis. Based on this, for internal phase-to-ground (PG) faults, during the simulations the A phase winding point to ground ranged between 5 and 95% with increments of 5%. On the other hand, for internal phase-to-phase (2P) and three-phase (3P) faults, grounded and ungrounded, the A phase winding point to B or/and C phases ranged between 5 and 95% with increments of 15%. Furthermore, the fault inception angle, considering the A phase current, was also varied to provide an in-depth performance analysis of the differential protection. The fault inception angles of 0° and 90° were considered. A solid fault resistance of 0.01 Ω was used in all cases, as the machine mechanical structure is usually solidly grounded [8]. According to the RTDS® manual, this is the minimum value that can be used in the simulation, which is related to sparse matrix issues.

In order to observe the loading condition influence, three wind speed values were considered, covering the WECS operating range. The values adopted in the simulations were: 12, 9 and 6 m/s.

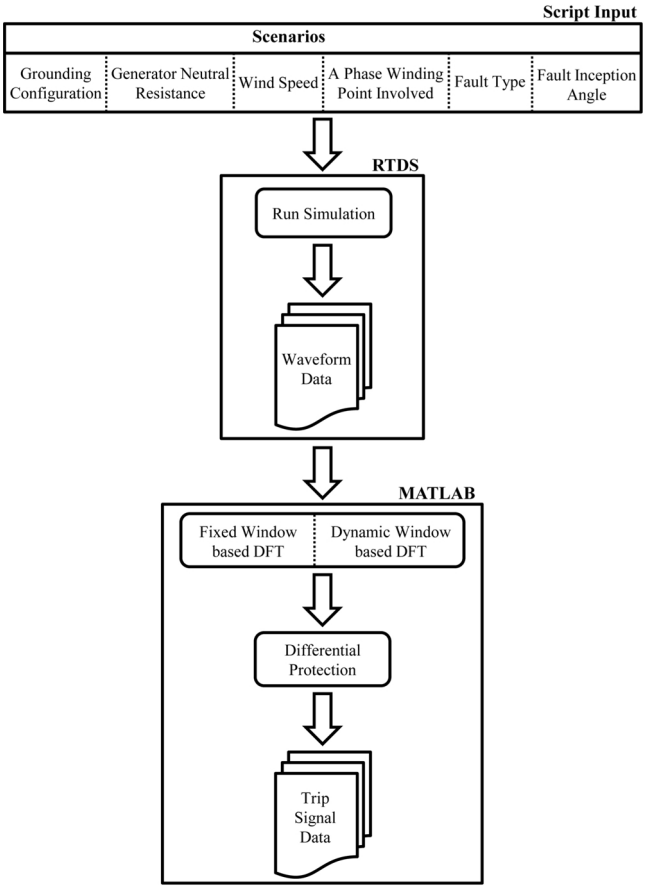

Fig. 6. Internal fault simulations methodology.

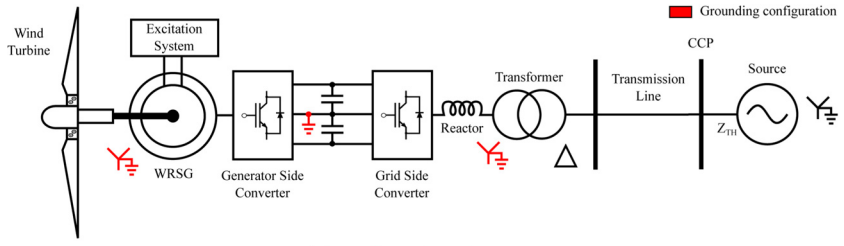

(a) EPS one-line diagram.

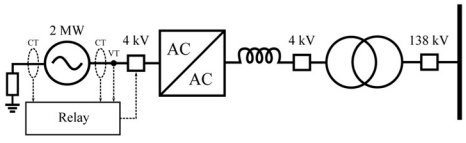

(b) Protection scheme.

Fig. 5. EPS modeled in RSCAD software.

Based on the defined scenarios, the simulation methodology to obtain the differential protection performance is summarized in Fig. 6. Basically, a script with all described scenarios was configured in the RSCAD software, RTDS® interface, to automatically run all simulations. The fault oscillographs were stored to be used as input in the protection performance test. The differential function, described in Section 2, was implemented using the MATLAB® R2015a software. Its input phasors were obtained using DFT with both window types described and analyzed in the previous subsection, enabling an additional analysis of the DFT accuracy influence.

The proposed protection scheme is based on two CTs per phase, as represented in Fig. 5(b). The adopted operating curve for the differential protection is based on Fig. 1 and the considered adjustments for its parameters Pickup 1, Slope 1, Base Point 1, Pickup 2, Slope 2 and Base Point 2 were 0.25 pu, 25%, 0.0 pu, 7.0 pu, 50% and 2.5 pu, respectively [8,22].

The results obtained from the proposed methodology are reported in the following subsection.

4.2. Simulation analysis

Table 3 summarizes the results for each grounding configuration scenario. It is important to mention that the results according to the fault inception angle are not presented in detail because the simulation showed that it has no impact on the differential protection performance. Considering the variation of the generator neutral resistance, wind speed, the A phase winding portion involved and fault inception angle, each of the scenarios 2, 4, 6 and 8 corresponds to 342 cases for A phase faults, 252 cases for phase-to-phase faults and 252 cases for three-phase faults, while each of the remaining contains 114 cases for A phase faults, 84 cases for phase-to-phase faults and 84 cases for three-phase faults, totalizing 4512 fault simulations.

The differential protection is adjusted to operate instantaneously in case of internal faults. Table 4 shows the tripping average time of this function, with a dynamic window based on DFT, to detect stator faults for each grounding configuration, as well as the variance and maximum/minimum values. The values obtained with a fixed window are represented between parentheses. As indicated, the detection time of this protection is extremely short and did not present a significant difference between grounding configuration scenarios and DFT window types.[1] It should be mentioned that the G30 relay has a frequency tracking mode [22]. The manufacturer's manual indicates that G30 differential function has a maximum operating time of 20 ms at 60 Hz, which increases for lower frequencies. Therefore, the proposed scheme has a similar operating time to a commercial relay for conventional applications.

As can be seen in Table 3, for internal phase-to-phase and three-phase faults, the differential scheme guarantees a complete protection of the stator winding for any grounding configuration. This occurs because these fault types result in a large system imbalance, which significantly increase the differential currents between phases near the machine's terminal and neutral.

On the other hand, in contrast to the differential protection performance for conventional applications, in which internal phase-to-ground faults near the neutral are unprotected and need a complementary protection (neutral overvoltage or third harmonic undervoltage functions) [8], its application for a full variable-speed wind generator with dq control shows that this function is suitable only when either the transformer or the back-to-back converter is grounded. If the control was dq0, this result would probably be similar to the conventional application, as the zero-sequence current path would be isolated between the grid and the generator sides by the power converter control. However, based on the literature, it can be inferred that the zero-sequence component is not considered in the wind generator control [28,5,29,26].

[1] Values obtained with a fixed window are represented between parentheses for the sake of comparison.

Table 3
Differential protection performance for each scenario.

Scenario	Fault Type	Correct operations	
		Fixed window [%]	Dynamic window [%]
1	PG	0	0
	PP and 3P	100	100
2	PG	78.36	80.70
	PP and 3P	100	100
3	All	100	100
4	All	100	100
5	All	100	100
6	All	100	100
7	All	100	100
8	All	100	100

Table 4
Tripping time of the differential protection.

Scenario	Mean [ms]	Variance [μs^2]	Maximum [ms]	Minimum [ms]
1	16.81 (16.09)[a]	40.09 (37.67)[a]	36.45 (30.46)[a]	4.41 (3.89)[a]
2	17.09 (15.92)[a]	58.96 (45.50)[a]	50.77 (47.90)[a]	3.37 (3.11)[a]
3	17.94 (17.00)[a]	41.15 (36.14)[a]	53.89 (40.61)[a]	4.15 (3.89)[a]
4	14.60 (13.74)[a]	73.05 (68.36)[a]	78.11 (76.81)[a]	3.11 (2.59)[a]
5	16.29 (15.32)[a]	43.11 (37.43)[a]	46.34 (47.90)[a]	4.15 (3.63)[a]
6	15.82 (14.94)[a]	41.27 (38.51)[a]	47.64 (44.26)[a]	3.37 (3.11)[a]
7	17.26 (16.40)[a]	45.62 (41.97)[a]	43.22 (33.06)[a]	4.68 (4.67)[a]
8	14.76 (13.88)[a]	65.07 (60.41)[a]	65.09 (63.79)[a]	2.59 (2.33)[a]

[a] Values obtained with a fixed window are represented between parentheses for the sake of comparison.

Based on the above, these grounding configurations, represented by scenarios 3 to 8, change the common path to ground of a typical generation unit (wye-grounded stator winding connected to a delta winding transformer or the opposite), helping the fault detection. This difference is exemplified in Figs. 7 and 8 , which consider identical internal faults near the neutral for scenarios 2 and 6, respectively.

For the case of scenario 2 represented in Fig. 7, the fault current behavior is similar to that of a conventional generation unit, as the machine terminal current decreases, the current near the neutral increases and the phase difference between I_1 and I_2 is small (20.6°). In this case, there is only one path to ground, which is the machine neutral resistance.

On the other hand, for the case of scenario 6 shown in Fig. 8, the machine terminal current increases due to the fact that the dq control scheme creates a ground path between the generator and transformer, resulting in a grid contribution to the fault current, that reflects in a large phase difference (72.2°), which facilitates the fault detection. This fault characteristic was presented by scenarios 3–8.

Furthermore, despite the fact that a fixed window based DFT introduces error in the phasor estimation, as previously presented, this characteristic resulted in a worse performance of the differential function only for the scenario 2, according to Table 3, that has a fault current behavior similar to a conventional generation unit. The detailed performance according to wind speed and machine neutral resistance is depicted in Table 5. It can be observed that, for this scenario, the lower wind speed and the higher neutral resistance result in a smaller protected winding portion. As the fault inception angle had no influence in the failure detection, the results were not detailed for this parameter.

Moreover, the worse performance mentioned only appeared for a wind speed of 6 m/s. It is a consequence of the small operating current and large frequency deviation from 60 Hz. Fig. 9 illustrates one of the cases of this occurrence. As can be seen, the phasor estimation error reflects in an oscillation of the currents' RMS magnitude, as well as in a

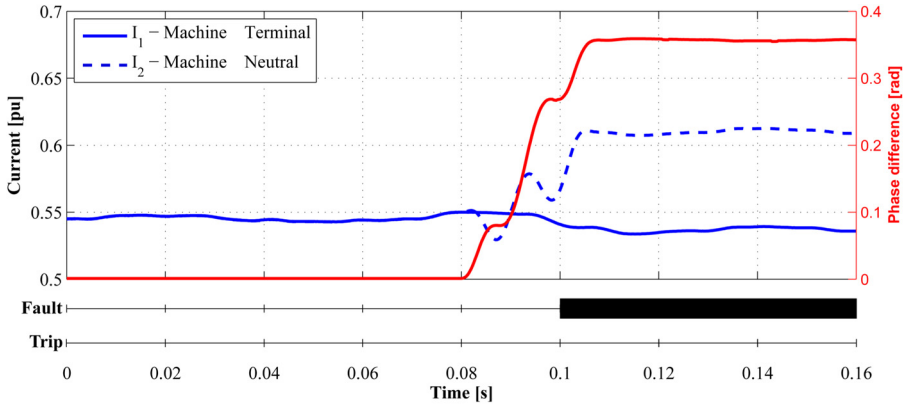

(a) RMS A phase currents near the machine's terminal and neutral.

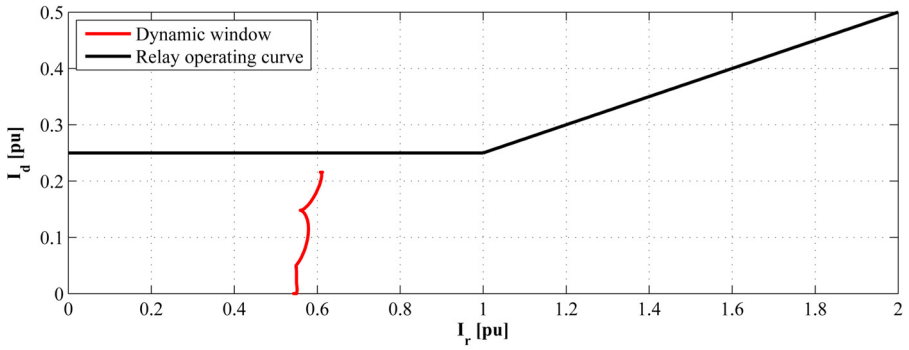

(b) Differential and restraint currents.

Fig. 7. Internal fault considering Scenario 2 with 9 m/s wind speed, 10% phase A winding point to ground, 3.1 Ω generator neutral resistance and 0° inception angle.

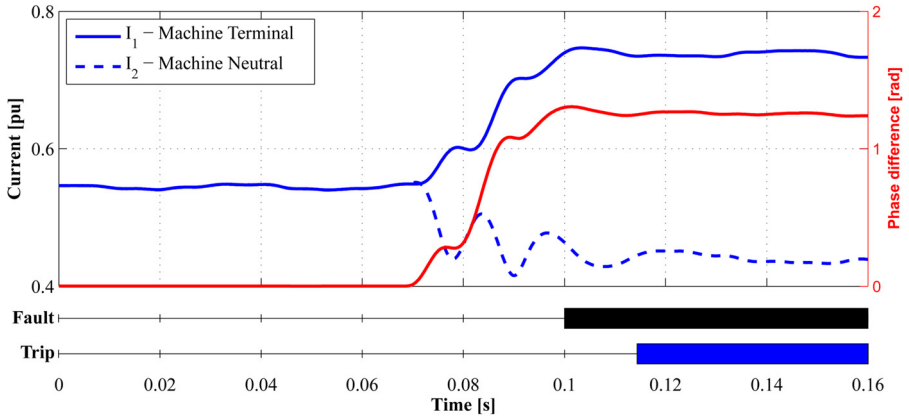

(a) RMS A phase currents near the machine's terminal and neutral.

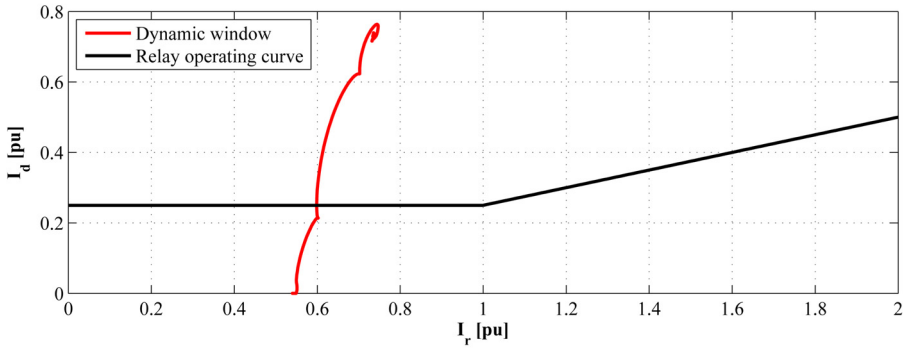

(b) Differential and restraint currents.

Fig. 8. Internal fault considering Scenario 6 with 9 m/s wind speed, 10% phase A winding point to ground, 3.1 Ω generator neutral resistance and 0° inception angle.

Table 5
Detailed differential protection performance in Scenario 2.

Condition		Correct operations	
Wind speed [m/s]	Generator neutral resistance [Ω]	Fixed window [%]	Dynamic window [%]
12	0.01	100	100
	3.1	94.74	94.74
	12.41	68.42	68.42
9	0.01	100	100
	3.1	89.47	89.47
	12.41	57.90	57.90
6	0.01	100	100
	3.1	78.95	84.21
	12.41	15.79	31.58

configuration should be avoided.

5. Conclusion

This paper has evaluated the application of the differential function in order to protect full-converter wind generators. The error introduced in the phasor estimation by a fixed window based on a DFT routine and the grounding configuration influence were investigated. The DFT performance tests show that a dynamic window must be used to guarantee a correct and safe operation of the protection system. The buffer size and sampling rate are specified according to the wind turbine operating range.

Considering dq control, simulation results show that for internal

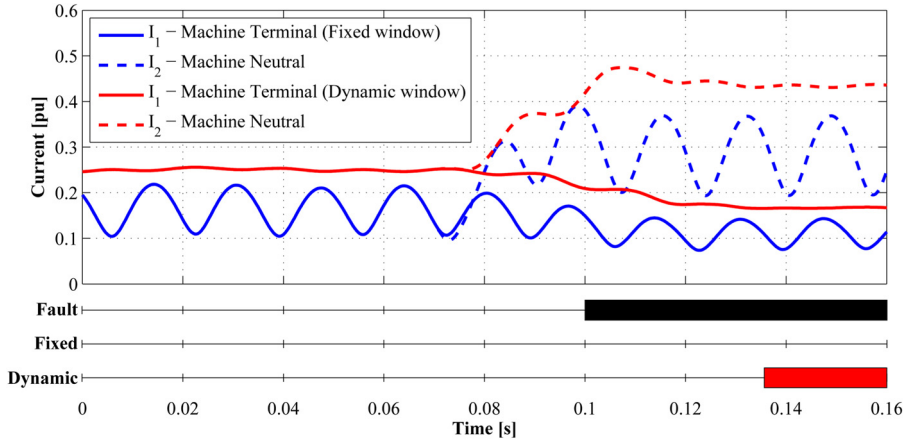

(a) RMS A phase currents near the machine's terminal and neutral.

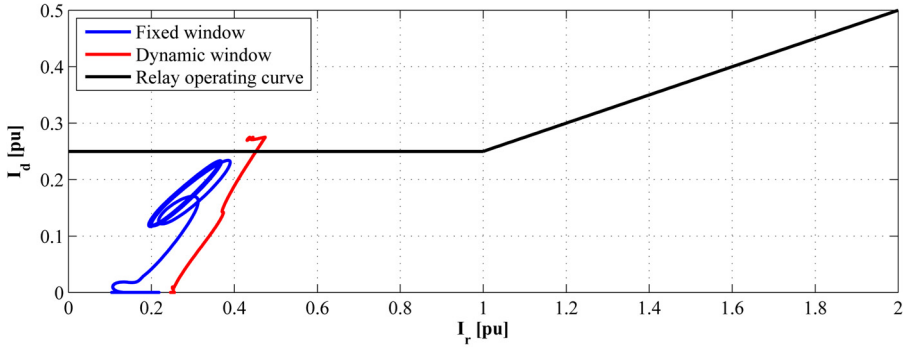

(b) Differential and restraint currents.

Fig. 9. Internal fault considering Scenario 2 with 6 m/s wind speed, 75% phase A winding point to ground, 12.41 Ω generator neutral resistance and 0° inception angle.

variation of the I_d and I_r values.

On the other hand, the fixed window based DFT was 100% accurate for the other scenarios, as well as the dynamic window based DFT. However, it is important to note that ideal CTs were used in the simulations. In other words, in a real situation, the error in phasor estimation may reflect in an improper operation because of CT errors. Hence, the results of this paper reiterate that the dynamic window based DFT must be used for a correct and safe operation.

Finally, another point is that all fault simulations with scenario 1 did not trip the differential function. This occurred because there is no ground path in this scenario. Therefore, the internal fault results in a neutral voltage displacement, as shown in Fig. 10. As illustrated, the phase under fault presents an undervoltage, whereas the healthy phases present an overvoltage. In these cases, the overvoltage relay would operate, however, as this function is delayed, the generator would be subject to a harmful condition temporarily. Thus, this grounding

phase-to-phase and three-phase faults, the differential protection ensures full protection of the stator winding for any grounding configuration. On the other hand, for internal phase-to-ground faults, the differential function had an accuracy of 100% when either the transformer or the back-to-back converter is grounded. These possible grounding configurations change the common path to ground of a typical generation unit (wye-grounded stator winding connected to a delta winding transformer or the opposite), facilitating fault detection. This is because the machine terminal current increases with a large phase difference to the current near the machine neutral. It is important to mention that the results were obtained with a typical adjustment of the differential function and the CT errors were not considered in the simulations.

Regarding the tripping time presented by the differential protection, it is extremely short, as observed for conventional applications, and did not present a significant difference between grounding configuration

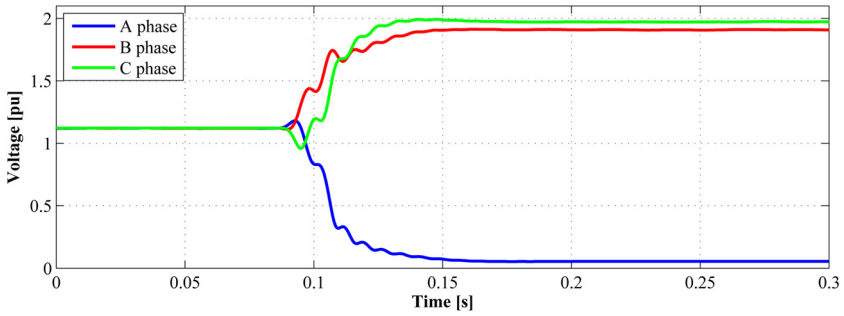

Fig. 10. Internal fault considering Scenario 1 with 12 m/s wind speed, 95% phase A winding point to ground and 0° inception angle.

Table 6
Controller parameters.

Converter	Variable	Controller	K_p	K_i
Grid-side VSC	i_{dg}	$G_{c,g}$	0.9000	79.9438
	i_{qg}	$G_{c,g}$	0.9000	79.9438
	u_{dc}	$G_{c,v}$	−0.5041	−6.7574
Generator-side VSC	i_{ds}	$G_{c,d}$	7.8300	695.5110
	i_{qs}	$G_{c,q}$	2.2632	127.3041
	ω_m	$G_{c,\omega}$	-5.4841×10^4	-3.2276×10^5
Exciter system	$i_{f,pu}$	$G_{c,f_{\text{pu}}}$	354.6450	3.1502×10^4

scenarios and DFT window type.

Finally, this paper corroborates the need to standardize and revise the protection functions for wind generators. Considering future work, it is important to embed the dynamic window based on DFT in order to analyze the processing time of the implemented algorithm. In addition, the grounding configuration impact on other protection functions applied for this WECS topology need to be studied and the development of a dq0 control scheme would be relevant to investigate its influence on fault current limitation.

Acknowledgments

The authors would like to thank the Power Systems Laboratory of the São Carlos School of Engineering, University of São Paulo, for the infrastructure provided, as well as the São Paulo Research Foundation (FAPESP), grants #2015/24028-7 and #2017/09554-0, and the Brazilian National Council for Scientific and Technological Development (CNPq), grant 456517/2014-6, for the financial support.

Appendix

The system data modeled in the RSCAD software for simulations in the RTDS® are presented below:

- **Grid:** S_{cc} = 1.1 GVA at an angle of 82°, V_{TH} = 138 kV, Z_{TH} = (2.409 + j17, 144) Ω, f_n = 60 Hz [30];
- **Transmission line:** $Z_L^+ = (0.357 + j0.5077)\,\Omega$/km, $Z_L^0 = (0.363 + j1.3262)\,\Omega$/km, Length = 10 km [31];
- **Transformer:** S_n = 2.5 MVA, 138 delta - 4 wye kV, Z_T = (0.005 + j0.04) pu [30];
- **Three-level voltage source converters:** Nominal power = 2 MVA, Grid-side reactor: L = 3.2 mH and R = 0.02 Ω, Nominal DC link voltage = 7.512 kV, DC link capacitor = 2.35 mF, f_{pwm} = 900 Hz [26];
- **Synchronous generator parameters:** S_n = 2 MVA, V_n = 4 kV, f_n = 60 Hz, P = 60, H_{gen} = 0.62 s, D = 0.01 pu, R_a = 0.006 pu, X_d = 1.3050 pu, X_q = 0.4740 pu, X'_d = 0.296 pu, X''_d = 0.252 pu, X''_q = 0.243 pu, X_l = 0.18 pu, X_0 = 0.13 pu, T'_{do} = 4.49 s, T''_{do} = 0.0681 s, T''_{qo} = 0.0513 s [26];
- **Turbine parameters:** Nominal mechanical power = 2 MW, rated wind speed = 12 m/s, cut-in = 6 m/s, cut-out = 25 m/s, H_{tur} = 4.32 s;
- **Control parameters:** The PI controllers gains, listed in Table 6, were adjusted according to the symmetrical optimum method, based on [26].

References

[1] GWEC, Global Wind Report – Annual Market Update, Global Wind Energy Council, Washington, USA, 2015.
[2] H. Li, Z. Chen, Overview of different wind generator systems and their comparisons, IET Renewable Power Generation 2 (2008) 123–138, https://doi.org/10.1049/iet-rpg:20070044.
[3] M. Glinkowski, J. Hou, G. Rackliffe, Advances in wind energy technologies in the context of smart grid, Proceedings of the IEEE 99 (2011) 1083–1097, https://doi.org/10.1109/JPROC.2011.2112630.
[4] V. Nelson, Wind Energy: Renewable Energy and the Environment, Taylor & Francis Group, LLC, New York, USA, 2009.
[5] O. Anaya-Lara, N. Jenkins, J. Ekanayake, P. Cartwright, M. Hughes, Wind Energy Generation: Modelling and Control, John Wiley & Sons, Ltd., West Sussex, UK, 2009.
[6] S.-G. Javier, L.-A. Roberto, Technological evolution of onshore wind turbines – a market-based analysis, Wind Energy 19 (2016) 2171–2187, https://doi.org/10.1002/we.1974.
[7] W.A. Elmore, Protective Relaying Theory and Applications, Marcel Dekker, Inc., New York, USA, 1994.
[8] IEEE, Guide for AC generator protection – redline, IEEE Std C37.102 (2007) 1–190.
[9] Y. Amirat, M. Benbouzid, E. Al-Ahmar, B. Bensaker, S. Turri, A brief status on condition monitoring and fault diagnosis in wind energy conversion systems, Renewable and Sustainable Energy Reviews 13 (2009) 2629–2636, https://doi.org/10.1016/j.rser.2009.06.031.
[10] J.F. Conroy, R. Watson, Low-voltage ride-through of a full converter wind turbine with permanent magnet generator, IET Renewable Power Generation 1 (2007) 182–189, https://doi.org/10.1049/iet-rpg:20070033.
[11] M. Khoddam, H. Karegar, Effect of wind turbines equipped with doubly-fed induction generators on distance protection, IEEE International Conference on Advanced Power System Automation and Protection (APAP), vol. 2, Beijing, China, 2011, pp. 1349–1353, , https://doi.org/10.1109/APAP.2011.6180588.
[12] T. Zheng, Y. Kim, P. Crossley, Y. Kang, Protection algorithm for a wind turbine generator in a large wind farm, PowerTech, IEEE/PES, Trondheim, Norway, 2011, pp. 1–6, , https://doi.org/10.1109/PTC.2011.6019337.

[13] A. Kusiak, W. Li, The prediction and diagnosis of wind turbine faults, Renewable Energy 36 (2011) 16–23.
[14] S.I. Gkavanoudis, C.S. Demoulias, A combined fault ride-through and power smoothing control method for full-converter wind turbines employing supercapacitor energy storage system, Electric Power Systems Research 106 (2014) 62–72, https://doi.org/10.1016/j.epsr.2013.08.007 URL: http://www.sciencedirect.com/science/article/pii/S0378779613002174.
[15] M. Mohapi, C. Buque, S. Chowdhury, Modelling and simulation of a protection scheme for a synchronous generator wind power plant, PES General Meeting | Conference Exposition, IEEE, Washington, DC, 2014, pp. 1–5, , https://doi.org/10.1109/PESGM.2014.6939055.
[16] A. Hooshyar, M. Azzouz, E. El-Saadany, Distance protection of lines connected to induction generator-based wind farms during balanced faults, IEEE Transactions on Sustainable Energy 5 (2014) 1193–1203, https://doi.org/10.1109/TSTE.2014.2336773.
[17] M. Mansouri, M. Nayeripour, M. Negnevitsky, Internal electrical protection of wind turbine with doubly fed induction generator, Renewable and Sustainable Energy Reviews 55 (2016) 840–855, https://doi.org/10.1016/j.rser.2015.11.023.
[18] R.P. Bataglioli, V.A.L. Freitas, D.V. Coury, R.M. Monaro, The influence of grounding configuration in a full conversion wind generator under internal faults, 2018 Power Systems Computation Conference (PSCC) (2018) 1–7, https://doi.org/10.23919/PSCC.2018.8443019.
[19] D. Reimert, Protective Relaying for Power Generation System, CRC Press Taylor & Francis Group, Florida, USA, 2006.
[20] B. Kasztenny, D. Finney, Generator protection and CT saturation problems and solutions, 58th Annual Conference for Protective Relay Engineers, Texas, USA, 2005, pp. 120–126, , https://doi.org/10.1109/CPRE.2005.1430427.
[21] IEEE, Guide for the application of current transformers used for protective relaying purposes, IEEE Std C37.110 14 (1999) 94–97, https://doi.org/10.1109/61.736693.
[22] G30 Generator Management Relay, 4.9x ed., Ontario, Canada, 2006.
[23] SIPROTEC Multifunction Machine Protection 7UM62 V4.6 Manual, 2017.
[24] S.H. Horowitz, A.G. Phadke, Power System Relaying, 3rd ed., John Wiley & Sons, Ltd., West Sussex, England, 2008.
[25] V. Madisetti, The Digital Signal Processing Handbook, CRC Press, 1997.
[26] L. Quèval, H. Ohsaki, Back-to-back converter design and control for synchronous generator-based wind turbines, 2012 International Conference on Renewable Energy Research and Applications (ICRERA), IEEE, Nagasaki, Japan, 2012, pp. 1–6, , https://doi.org/10.1109/ICRERA.2012.6477300.
[27] R.M. Monaro, Fuzzy Logic Applied in Synchronous Generators Digital Protection Improvement, São Carlos School of Engineering – University of São Paulo, Brazil, 2013 Ph.D. Thesis.
[28] A. Yazdani, R. Iravani, A neutral-point clamped converter system for direct-drive variable-speed wind power unit, IEEE Transactions on Energy Conversion 21 (2006) 596–607, https://doi.org/10.1109/TEC.2005.860392.
[29] B. Wu, Y. Lang, N. Zargari, S. Kouro, Power Conversion and Control of Wind Energy Systems, John Wiley & Sons, Hoboken, NJ, 2011.
[30] W.H. Kersting, Radial distribution test feeders, IEEE Transactions on Power Systems 6 (1991) 975–985, https://doi.org/10.1109/59.119237.
[31] A. Hooshyar, M.A. Azzouz, E.F. El-Saadany, Distance protection of lines emanating from full-scale converter-interfaced renewable energy power plants – Part I: Problem statement, IEEE Transactions on Power Delivery 30 (2015) 1770–1780, https://doi.org/10.1109/TPWRD.2014.2369479.